LAWRENCE
LIVERMORE
NATIONAL
LABORATORY

LLNL-CONF-695681

Technique for diamond machining large ZnSe grisms for the Rapid Infrared/Imager Spectrograph (RIMAS)

P. J. Kuzmenko, S. L. Litle, A. S. Kutyrev, J. I. Capone

June 23, 2016

SPIE Advances in Optical and Mechanical Technologies for Telescopes and Instrumentation
Edinburgh, United Kingdom
June 26, 2016 through July 1, 2016

Disclaimer

Technique for diamond machining large ZnSe grisms for the Rapid Infrared/Imager Spectrograph (RIMAS)

Paul J. Kuzmenko*[a], Steve L. Little[a], Alexander S. Kutyrev[b,c] and John I. Capone[c]

[a]Lawrence Livermore National Laboratory, L-183, PO Box 808, Livermore, CA 94551;
[b]NASA Goddard Space Flight Center, 8800 Greenbelt Rd., Greenbelt, MD, 20771;
[c]Dept. of Astronomy, Univ. of Maryland/College Park, Stadium Drive., College Park, MD 20771

ABSTRACT

The Rapid Infrared Imager/Spectrograph (RIMAS) is an instrument designed to observe gamma ray burst afterglows following initial detection by the SWIFT satellite. Operating in the near infrared between 0.9 and 2.4 μm, it has capabilities for both low resolution (R~25) and moderate resolution (R~4000) spectroscopy. Two zinc selenide (ZnSe) grisms provide dispersion in the moderate resolution mode: one covers the Y and J bands and the other covers the H and K. Each has a clear aperture of 44 mm. The YJ grism has a blaze angle of 49.9º with a 40 μm groove spacing. The HK grism is blazed at 43.1º with a 50 μm grooves spacing.

Previous fabrication of ZnSe grisms on the Precision Engineering Research Lathe (PERL II) at LLNL has demonstrated the importance of surface preparation, tool and fixture design, tight thermal control, and backup power sources for the machine. The biggest challenges in machining the RIMAS grisms are the large grooved area, which indicates long machining time, and the relatively steep blaze angle, which means that the grism wavefront error is much more sensitive to lathe metrology errors. Mitigating techniques are described.

Keywords: grism, RIMAS, diamond machining, ZnSe, immersion grating

1. INTRODUCTION

RIMAS (the Rapid Infrared Imager/Spectrograph)[1] is an instrument being built for installation on the 4 meter Discovery Channel Telescope[2] in Happy Jack, AZ. It is a target of opportunity instrument specifically designed to capture photometric and spectral data from the afterglow of gamma ray bursts. Such bursts are believed to be associated with the collapse of supernova or the merging of binary neutron stars[3]. Upon detection of a gamma ray burst by the orbiting SWIFT satellite, the location of the burst can be localized to within a few arc seconds in just over one minute and relayed down to the ground. The telescope can then be rapidly slewed to point RIMAS to the source of the gamma radiation.

RIMAS is designed to cover the spectral range of 0.9 to 2.4 μm in two channels. The emphasis on the infrared is to accommodate the large red shifts of distant objects as well as providing improved transmission through interstellar dust. A dichroic mirror (see figure 1) directs light to either the short wavelength channel covering the Y and J bands (0.97 - 1.07 μm and 1.17 - 1.33 μm) or the long wavelength channel covering the H and K bands (1.49 - 1.78 μm and 2.03 - 2.37 μm). A rotating wheel in each pupil plane allows the insertion of filters and grisms. RIMAS has both a low resolution spectral mode (R~25) and a moderate resolution mode (R~4000). Low resolution dispersion is provided by calcium fluoride grisms operating in first order. Moderate resolution is achieved with diamond machined ZnSe grisms operating in high order used in conjunction with ZnSe prism cross-dispersers.

LLNL has previous experience machining grisms[4] and immersion gratings[5] in zinc selenide using the Precision Engineering Research Lathe (PERL II). We were asked to produce the moderate resolution grisms for RIMAS. This paper will discuss the fabrication technique. Section 2 presents the optical and mechanical specifications for the grisms

*kuzmenko1@llnl.gov: phone 925-423-4346; fax 925-422-2499

with their tolerances. Section 3 describes the precision lathe, the diamond tool, the design of the machining fixture and the preparation of the grism blanks. Previous efforts in machining ZnSe gratings are reviewed in section 4. Challenges anticipated in the fabrication and possible means of their mitigation are discussed in section 5. We conclude in section 6 by outlining the next steps in the fabrication process.

2. GRISM SPECIFICATIONS AND TOLERANCES

Unlike prisms, a grism produces spectral dispersion without deviating the path of the incident beam. Therefore they can be inserted in a filter wheel near the pupil plane to add spectral capability to an imager. The dispersion and spectral resolution of a grism scales as (n-1), where n is the refractive index of the grism substrate. Of readily available optical materials with good transmission in the 0.9 to 2.4 μm range, zinc selenide has the highest refractive index and hence provides the greatest spectral resolution. So RIMAS was designed to incorporate ZnSe grisms.

Details of the optical design have been presented elsewhere[6,7]. The optical specifications of the two ZnSe grisms are shown in Table 1.

Table 1. Optical specifications of the YJ and HK grisms. Values are specified at room temperature.

Grism	Wavelength (μm)	Grooves/mm	α wedge (deg)	Θ blaze angle	Diffraction orders
(1) YJ band	0.9-1.35	25	43.075	43.075	30 - 44
(2) HK band	1.5-2.35	20	49.926	49.926	23 - 39

The beam diameter is 40 mm at the entrance face. Since the exit face is inclined by the apex angle the beam footprint is elliptical extending nearly 55 mm for the YJ grisms and just over 63 mm for the HK. The grisms are sized so that the beam footprint covers 90% of the clear aperture, by which we mean the ruled area, and 80% of the physical area of the grism surface. See figure 2 for a side view of the grism showing incident and apex angles along with the incident beam.

The prism apex angle and grism blaze angle must meet the above specifications to within ± 0.1º. The apex angle is set by the geometry of the machining fixture and the blaze is set by the angle of the cutting face of the diamond tool.

To achieve the desired spectral resolution over the full wavelength range the transmitted wavefront error should be less than one wave peak to valley at 1 μm wavelength with a goal of 1/2 wave peak to valley. When measured at 633 nm, the surface error of the groove facets should be less than 0.48 λ to meet the requirement and 0.24 λ to meet the goal.

Periodic error in groove spacing generates ghosts, spurious artifacts in the detected spectra that can make interpretation of the data difficult. RIMAS needs a ghost intensity of less than 1% of the intensity of the peak diffracted order. The intensity of scattered light from the grisms should be less than 0.1% of the intensity of the peak order. This can be attained with a groove surface roughness of ≤7 nm rms for the YJ grism and ≤10 nm rms for the HK grism.

The groove apex angle (i. e. angle between the groove facets) should be chosen to attain the highest possible diffraction efficiency. One might expect that a 90º apex would be best as that would minimize groove shadowing effects. To verify intuition we modeled the grisms using a one dimensional RCWA (rigorous couple wave analysis) vector code[8] in MATLAB. We validated the code by comparing its output with the results of previous calculations done in GD-Calc and GSolver on other gratings and grisms. A second check was to model the Ohio State University instrument OSMOS. The MATLAB output was consistent with the measured efficiency data.

Efficiency calculations were done for order 36 of the YJ-grism. The calculation assumes an incident field within the grism substrate (i.e ignoring reflection at the entrance face of the grism). We took the wavelength dependent refractive index for ZnSe at 80 K from the Leviton et al.[9] 2005 CHARMS paper. The angled groove surfaces are modeled by a stairstep profile. A step size of 0.1 μm (300 steps) produced good convergence. We assumed a wave with TE polarization incident on the grating surface at the prism angle of 43.075 degrees. The results shown in figure 3 indicate that a 90º groove apex angle is indeed optimal.

3. DETAILS OF FIXTURING AND MACHINING

3.1 Fixture design

Proper fixture design is critical to the success of a precision machining operation. A fixture is the interface between an unfinished optical blank and the machine that will give it its final precise shape. We require that the blank be held in a stable and secure manner. The part should be held in a stress-free condition so that there is no "springing back" and consequent surface distortion once removed from the fixture. It is recommended that the same mount points and clamping forces be used in the machining fixture as will be used to hold the part in the optical instrument. The configuration of our diamond turning lathe is such that the plane of the gratings that it cuts is horizontal. So the surface to be machined surface must be held horizontal in the fixture.

We addressed this issue by providing mounting surfaces on the grism blanks. These take the form of support rails ground into the blank as shown in figures 4 and 5. By recessing the top surface of the rail about a millimeter below the grating surface, the groove length only needs to equal the width of the clear aperture. This eliminates unnecessary machining time.

While resting in the fixture there is no net force on the blank other than the downward force of gravity. A cyanoacrylate adhesive (Loctite 495) is used to bond the blank to the fixture at 3 raised pads along the fixture rails (2 along one rail and 1 along the other rail). Care is taken that the blank and the fixture are in thermal equilibrium with the environment inside the machine enclosure when bonded so that no thermally induced stresses are locked in by the adhesive. Figure 6 shows the HK blank resting in its fixture. The fixture uses a common base, so only the support insert is changed to machine a different grism.

Even though there is tight temperature control in the machining environment it is good practice to match the coefficients of thermal expansion (CTE) of the fixture and the machine structure. In our case most of the machine, including the rails, hydrostatic bearings and the stages are constructed of 17-4 PH stainless steel which has a CTE of 10.5×10^{-6}/ºC near room temperature. The machining fixture is made from 1018 low carbon steel with a CTE of 10.9×10^{-6}/ºC.

There is an unavoidable mismatch between the ZnSe blank (CTE~7.1×10^{-6}/ºC) and the steel in the fixture and the machining structure. We can reduce the effects of differential expansion by keeping the support rails no thicker than necessary. In the RIMAS blanks the rails are 6 mm thick and their lower surface is only 7 mm below the top of the blank.

3.2 Optical blank preparation

Proper surface preparation of the grism blank is necessary to ensure that it is free of subsurface damage. This damage occurs when the substrate is ground or polished with abrasive. Microcracks extend beneath the surface a distance that depends on the particle size of the abrasive used. If microcracks are present and the depth of cut is less then the depth of the damaged layer, then the material will tend to yield along those cracks rather than along the direction of the diamond tool cut.

Ohta[10] and his colleagues have shown that in silicon and germanium the subsurface damage extends a depth of 3 times the maximum value of the surface roughness and that the maximum roughness of a ground surface varies logarithmically with abrasive size. We expect similar results for zinc selenide.

We have had inconsistent results in obtaining damage-free ZnSe from several sources. So it is important to obtain a sample polished by a prospective vendor and verify the material quality with a test cut. F1 Optics Inc. prepared a one inch diameter ZnSe disc into which we machined grooves. The grooves were clean and sharp with no evidence of chipping. Then we were able to procure the grism blanks. Rough ZnSe grism blanks were supplied II-VI, Inc. They were shaped to final form and polished by F1 (see figure 4).

3.3 PERL II diamond turning machine

LLNL's PERL II (shown in figure 7) is a numerically controlled 2-axis precision lathe. It was constructed in 1984 to advance the state of the art in machine tool technology and has been used since 2002 to fabricate immersion gratings and grisms in infrared transmitting materials. Gratings are cut with the machine set up as a flycutter. A diamond tool is set into the horizontal axis spindle and rotated while the grating blank in translated beneath cutting a groove, as shown in figure 8.

Two ultra-stiff linear hydrostatic slides with a nominal 10 cm range of travel are mounted on a 46 cm thick granite base. One slide translates the spindle and its drive motor; the other translates the workpiece. Laser interferometers control position with 2.54 nm resolution. The granite base is supported on pneumatic isolators. These isolators worked well enough that machining of a grating continued uninterrupted during a shallow (0.5 km depth) magnitude 3.0 earthquake centered just over 4 km from the machine.

One key to the long term mechanical stability of PERL II machine is tight temperature control. The room surrounding PERL is temperature controlled to ±0.25ºC. The machine itself sits inside an aluminum and Plexiglass enclosure that has a recirculating downdraft airflow that is controlled to ±0.005ºC. A reservoir of light mineral oil used as a cutting fluid and coolant resides in the same enclosure and hence is controlled to the same temperature. The major heat source in the enclosure is the spindle motor. It is enclosed in a cooling water jacket. The water temperature is regulated to 0.01ºC.

PERL uses a capstan drive to translate the X-axis and Z-axis stages. We have found through experience that despite the hydrostatic bearings on the rails we experience a slight but consistent transverse displacement between forward and reverse motion along a rail. This displacement shift of order 120 nm between grooves produces a periodic error in the groove spacing when grooves are cut with a back and forth motion. As a result Rayleigh ghosts are present at the midpoint between diffraction orders. Ghost intensity is roughly 1% of the peak diffraction intensity at visible (HeNe) wavelengths. The remedy is to cut grooves only in one direction, moving the tool completely around the part before beginning the next groove. When this is done the intensity of the Rayleigh ghosts falls to less than that of the grating scatter. The penalty for unidirectional cutting is an increase in the machining time of roughly 30 to 40% compared with a back and forth cut.

3.4 Diamond tool specification

In our flycutting process the shape of the diamond tool tip is duplicated in the shape of the groove. Since the tool is mounted vertically in the spindle as it cuts a groove, the blaze angle (angle of the blazed facet relative to the plane of the grating) is the angle of the cutting surface of the tool relative to horizontal. This angle will be 43.1º for the YJ grism and 49.9º for the HK grism. The tool apex angle, which sets the angle between the grating facets, has been determined to be 90º for highest efficiency. Calculations and previous tests have shown that the diffraction efficiency is highest over the broadest spectral range when the groove facets are flat and hence the cutting edges of the diamond are straight. From this it follows that the tip of the diamond tool should be as sharp as possible as that maximizes the flat area of the groove. We have cut gratings in germanium in which the corner radius at the base of the groove was less than 0.1 μm[11].

A final step is to specify the rake angle of the tool. Like other brittle optical materials, zinc selenide is optimally cut with a negative rake tool, which puts the material into compression. The high pressures produced by the negative rake and the small contact area, as a result of reducing the feed rate to obtain a very small uncut chip thickness, enables ductile mode machining. We have found that a 30º negative top rake angle that works well with germanium also works well with zinc selenide. Since we need cleanly cut surfaces on both facets of the groove a tool with a double negative rake angle (each cutting face has a negative rake) is required. See figure 9 for a drawing and a photo of the diamond tool to be used.

4. PREVIOUS GRATINGS MACHINED IN ZINC SELENIDE

Our first test grating in ZnSe was machined at LLNL in 2006[12]. We cut 2 mm segments of 30 μm pitch grooves into a polished ZnSe window at feed rates varying from 0.1 to 1.0 inch/minute to determine the optimal cutting conditions. A rate of 0.4 inch/minute was the highest value at which good quality grooves could be observed. Tests showed an rms groove roughness of 5 nm. The surface error in the grating was 0.30λ peak to valley and 0.030λ rms measured at 633 nm.

A large immersion grating was attempted as a prototype optic for the WINERED spectrograph[13]. The grating area was an order of magnitude larger than the previous grating. Much was learned about proper preparation of the surface of the blank, proper fixturing and improving the reliability of PERL to support long machining times.

The most recent grating machined in ZnSe was a grism made for the Canadian NIRISS instrument onboard the JWST[4]. This had a 30 x 29 mm clear aperture on a wedged substrate whose thickness varies from 5 mm to 11 mm. Figure 10 shows the grating blank fixed in PERL just before the start of machining. This grism had a 2.6º blaze. Its surface error was quite low, 0.21λ peak to valley and 0.030λ rms over the full aperture at 633 nm. The diffraction pattern was very clean with no visible ghosts due to unidirectional cutting. We observed a diffraction efficiency of 56% at 633nm for the uncoated grism. Optical profilometry measured a groove roughness of about 3 nm rms so the scatter was very low. If we can achieve similar performance from the RIMAS grisms they would meet all their requirements.

5. CHALLENGES

There are several challenges that must be overcome to produce satisfactory grisms for RIMAS. This will be the largest area grating that we have machined in ZnSe. The grating area measures 45 x 60 mm for the YJ grism and 45 x 70 mm for the HK grism. By comparison the previously machined gratings for NIRISS measured 29 x 30 mm and for WINERED 50 x 58 mm. On the other hand the groove spacings of 40 μm and 50 μm for the RIMAS grisms are larger than for these other gratings (NIRISS 18.42 μm, WINERED 31.7 μm). As a result the total length of the grooves to be cut, which determines machining time, is only about 10% greater than for the NIRISS grism. Machining time may be estimated from the total length of the grooves and the nominal feed rate of 0.35 to 0.4 inch/minute. For unidirectional cutting, as will be implemented here to greatly reduce grating ghosts, the machining time increases by 35 to 40% to account for the tool motion around the part to reposition the tool for the start of the next groove. We estimate a machining time of about 150 hours for each of the RIMAS grisms. This is small compared to machining time of 670 hours for a large germanium immersion grating completed in late 2015[14].

Long machining times can stress the reliability of PERL as many systems need to function flawlessly. We lost one of the WINERED gratings 2/3 of the way through its cut when an electrical brownout occurred. Although the building lights dimmed for only a fraction of a second the undervoltage was enough to halt the control computer and cause metrology to be lost. We have since installed uninterruptable power supplies on all the electronic systems in PERL Unfortunately they do not have enough capacity to power the chillers supplying cooling water to the machine enclosure or to the spindle. But the chiller controls are set to restart once power is restored, so a short interruption could be tolerated.

The increased blaze angles Θ_B of 43º and 50º vs. 2.6º for the NIRISS grism present another challenge. Consider the coordinate system shown in figure 8, where Z is the direction along the spindle axis, X is orthogonal to the spindle axis and in the horizontal plane (i.e. along the grooves) and Y is orthogonal to the spindle axis and vertical. A groove position error along the spindle axis, Δz, results in a surface error $(\Delta z)\sin\Theta_B$ along the optical beam. Position errors can have several causes. The laser interferometer measures the position of the spindle bearing relative to a reference corner cube. It cannot detect changes in spindle length caused by temperature changes inside the machine enclosure. The laser interferometer is not compensated for changes in refractive index along the beam path due to changes in atmospheric pressure or humidity. So changes in the fringe position due to a change in refractivity will be misinterpreted as spindle motion and generate an erroneous position correction. Due to the increased blaze angle the surface error for the RIMAS grisms will be about 16 times greater than that of NIRISS for the same Δz. One can estimate the effect upon the grating surface error of changes in barometric pressure. In the worst case with the spindle fully extended there is a 25 cm path length difference L between the two arms of the laser interferometer. A change in pressure of 4 millibars (a good day) will shift the refractive index Δn by about 1.07×10^{-6}. This shifts the fringes by $L\Delta n$, which translates to a 0.27 μm error

in groove position. The error can be much less with the spindle near minimum extension, L= 5 cm, but much greater on a stormy day with pressure changes of up to 20 millibar.

There are several possible mitigations for the lack of barometric pressure compensation. A simple one would be to establish limits on the allowable range of pressure and pause machine motion when those limits are exceeded. One can use long range weather forecast models available online to select an opportune time to start machining. Northern California is known for very stable summertime weather patterns. The period from May through September is an especially good time to machine gratings. Knowing that confidence in predicted pressures decreases as the forecast period extends one can begin machining with the spindle at its maximum required extension. This corresponds to the maximum path length difference in the z-axis laser interferometer and the position of greatest sensitivity to pressure changes. But as the spindle moves in as machining proceeds, the sensitivity will continually decrease.

6. NEXT STEPS

Having acquired the diamond tools, grism blanks and the machining fixtures we are ready to fabricate the RIMAS grisms. The first step is to test the diamond tools to verify that the grism blaze angle will be correct. We will also need to see that the tool cuts high quality chip-free grooves. So we first cut a test grating on a germanium blank (one inch diameter disc). Germanium is used because tool wear in germanium is very low and it machines well under the same conditions that work for zinc selenide. The diffraction pattern is observed in reflection with a 633 nm HeNe laser. We measure the angles of diffraction of the various orders and the intensities of each. The two brightest orders are located and the blaze angle is evaluated by interpolating between the diffraction angles of those orders using the method of Loewen and Popov[15]. This method assumes that the diffracted intensities vary as those from perfectly flat and smooth grooves. One should verify this by measuring the intensities of a number of orders. If the grooves are not flat then the incident optical power will be distributed over a wider range of orders, which reduces the peak diffraction efficiency. The measured blaze angle should match the specification to within 0.1º. If this is not the case then it is possible to adjust the blaze by grinding a correction on the vertical reference surface on the tool shank. This tilts the grating slightly in the holder thereby modifying the blaze angle of the grooves that it cuts. Another germanium blank must be recut with the modified tool to verify that the correct blaze angle has been achieved.

The germanium test grating is inspected under an optical microscope to verify groove quality. The flatness of the groove facets is tested using an optical profilometer or an atomic force microscope. If the groove flatness is poor then the diamond tool needs to have the cutting edge reworked or else another tool must be used.

At this point a test grating is cut on a small ZnSe blank (one inch diameter disc), which has been polished damage-free using the same technique used to prepare the grism blanks. This test grating will have the same groove period as the actual grism and be cut using the same machining parameters (1000 rpm spindle, unidirectional feed 0.35 inch/minute) to be used on the actual grisms. As with the germanium visual inspection under an optical microscope and optical profilometry are performed to verify that the groove quality is satisfactory. The diffraction pattern is measured to check the blaze angle and the diffraction efficiency.

Having successfully produced a test grating in ZnSe, we are ready to machine the RIMAS grisms. The fixture is first test fit into PERL. If the test fit is successful both blank and fixture are allowed to come to thermal equilibrium inside the machine enclosure. Then the grism blank is secured to mounting pads on the fixture with cyanoacrylate adhesive. The blank is held in a special handling fixture that insulates it from body heat of the worker securing into the machining fixture. Next the machining fixture is mounted onto the PERL translation stage and adjusted so that its edges are parallel to the machine axes and the surface is level to within 1 μm. The diamond tool is mounted to the spindle and the position of the tool tip set to achieve the proper depth of cut into the surface of the blank, approximately 15 μm. In parallel the numerical control instructions are generated, tested and loaded into the control computer. The PERL instructions are simply a set of points that specify the successive tool locations during the machining process. A spray of light mineral oil at a flow rate of around 20 mL/hour is directed onto the workpiece and the PERL spindle is started. The machine pauses for 12 hours reaching full thermal equilibrium before motion of the axes is started and the machining commences. In approximately 150 hours the machining is completed. The grism is removed from the machine, cleaned of all oil and machining residue, and given a visual inspection. It is now ready for testing.

Several tests will be conducted to demonstrate that the grisms meet their design specification. Observation of the diffraction pattern and measurements of the diffraction efficiency are the most important. One will also measure the intensity of grating ghosts and grating scatter. Wavefront error is also important to measure as that can limit the spectral resolution. Finally the grisms are ready for a 0.9 to 2.4 μm antireflection coating on the entrance face. Then installation in RIMAS can occur.

ACKNOWLEDGEMENTS

Thanks are owed to Steve Bond, Steve Bretz, Rich Cobiseno and the Machine Tool Services Group, Pete Davis, Dave Hopkins, Travis Martin, Mario Montoya, Jim Morton, and Darron Nielsen for their work over a number of years in keeping PERL II operating. Thanks to Rick Montesanti for helpful discussions. Brian Yoxell provided the fixture design. Thanks to Melinda Lane, Wilthea Hubbard and Peter Haugen in the National Security Engineering Division and Bonnie Zucca of the Global Security directorate at LLNL for covering the expenses of attending this conference. This work was performed under the auspices of the U.S. Department of Energy by Lawrence Livermore National Laboratory under Contract DE-AC52-07NA27344.

REFERENCES

[1] Kutyrev, A. S. et al., "RIMAS: infrared imager-spectrometer for the Discovery Channel Telescope," Proc. SPIE 9908, (2016).
[2} Gehrels, N., Ramirez-Ruiz, E. and Fox, D. B., "Gamma-Ray Bursts in the Swift Era," Annu. Rev. Astron. Astrophys. 47(1), 567-617 (2009).
[3] Levine, S.E., et al., "Status and performance of the Discovery Channel Telescope during commissioning," Proc. SPIE 8444, 844419 (2012).
[4] Kuzmenko, P. J., Little, S. L., Albert, L. Aldridge, D. A., Doyon, R., Maszkiewicz, M., and Touahri, D., "Diamond machining of ZnSe grisms for the Near Infrared Imager and Slitless Spectrograph (NIRISS) onboard JWST," Proc. SPIE 9151, 915159 (2014).
[5] Ikeda, Y., Kobayashi, N., Kuzmenko, P. J., et al., "ZnSe immersion grating in the short NIR region", Proc. SPIE Vol. 9151, 915144 (2014).
[6] Capone, J. I., et al., "Cryogenic optical systems for the rapid infrared imager/spectrometer (RIMAS)," Proc. SPIE 9147, 914736 (2014).
[7] Capone, J., Content D. A., and others, "The development and analysis of cryogenic optical systems for the rapid infrared imager/spectrometer," Proc. SPIE 8863, (2013).
[8}https://sourceforge.net/projects/rcwa-1d/
[9] Leviton, D. B., Frey, B. J. and Kvamme, T., "High accuracy, absolute, cryogenic refractive index measurements of infrared lens materials for JWST NIRCam using CHARMS," Proc. SPIE 5904, 59040O (2005).
[10] Ohta, T., Yan, J., Kuriyagawa, T., Kodera, S. and Nakasuji, T., "Prediction of subsurface damage depth of ground brittle materials by surface profiling," Int. J. Machining and Machinability of Materials, 2(1), 108-124 (2007).
[11] Kuzmenko, P. J., Davis, P. J., Little, S. L., Little, L. M. and Bixler, J. V., "High efficiency germanium immersion gratings," Proc. SPIE 6273, 62733T (2006).
[12] Kuzmenko, J. P., Little, S. L., Ikeda, Y., and Kobayashi, N., "Fabrication and testing of diamond-machined gratings in ZnSe, GaP, and bismuth germanate for the near infrared and visible," Proc. SPIE 7018, 70184Q (2008).
[13] Kuzmenko, P. J., Little, L. M., Ikeda, Y., and Kobayashi, N., "Progress in the fabrication of a prototype ZnSe immersion grating for the WINERED spectrograph," Proc. SPIE 7739, 7739U (2010).
[14] Montesanti, R., Little, S. L., Kuzmenko, P. J., et al.," Strategies for single-point diamond machining a large format germanium blazed immersion grating," Proc. SPIE 9912, (2016).
[15] Loewen, E. G. and Popov, E., [Diffraction Gratings and Applications], Dekker, New York, 420 (1997).

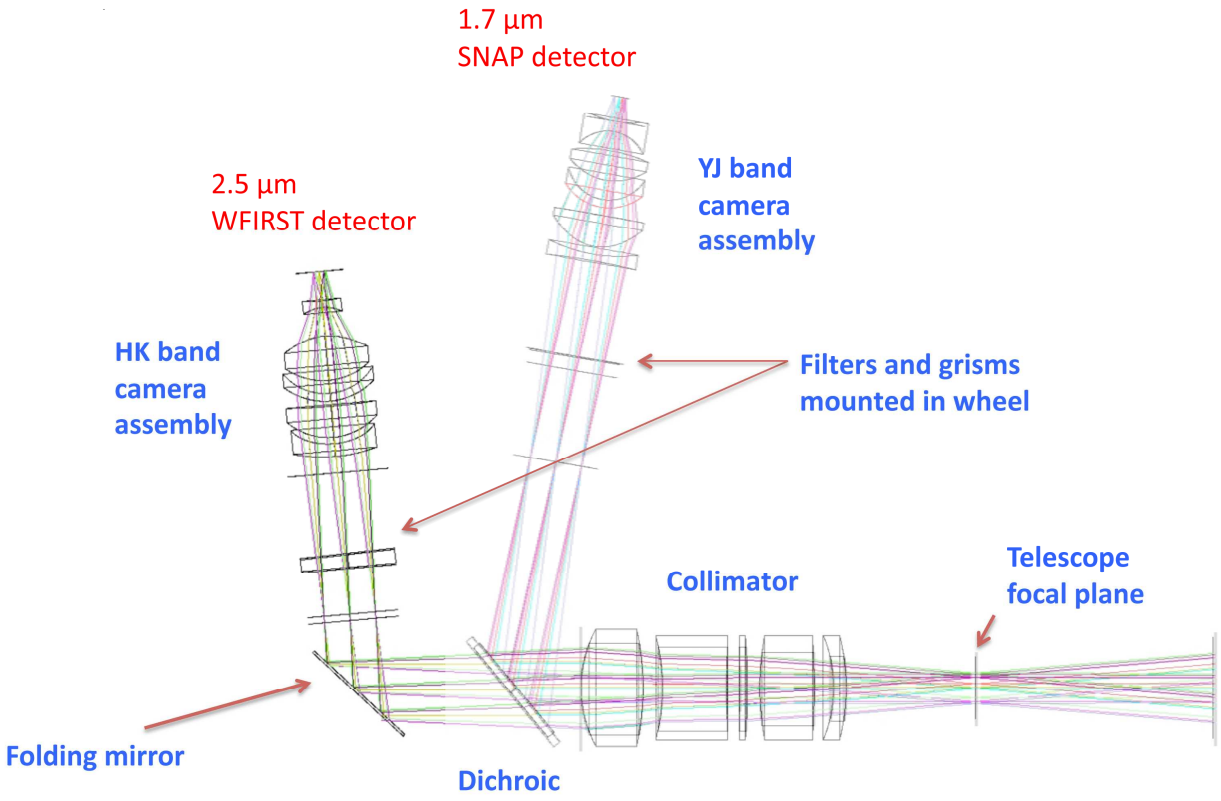

Figure 1. This is the optical layout of the RIMAS instrument showing its two spectral channels with separate detectors and separate filters and grisms. The beam is 40 mm in diameter at the pupil.

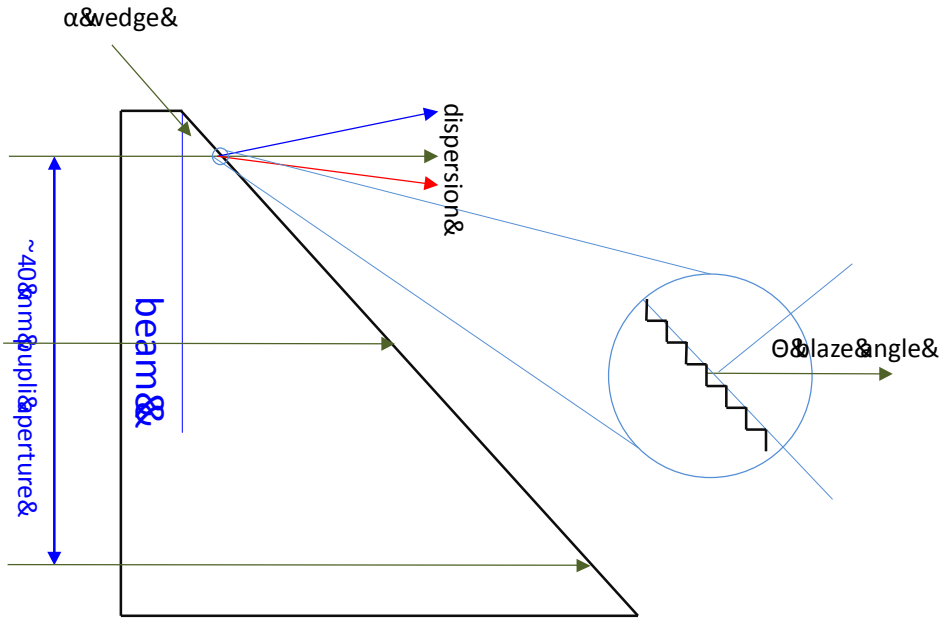

Figure 2. Profile view of grism showing incident beam

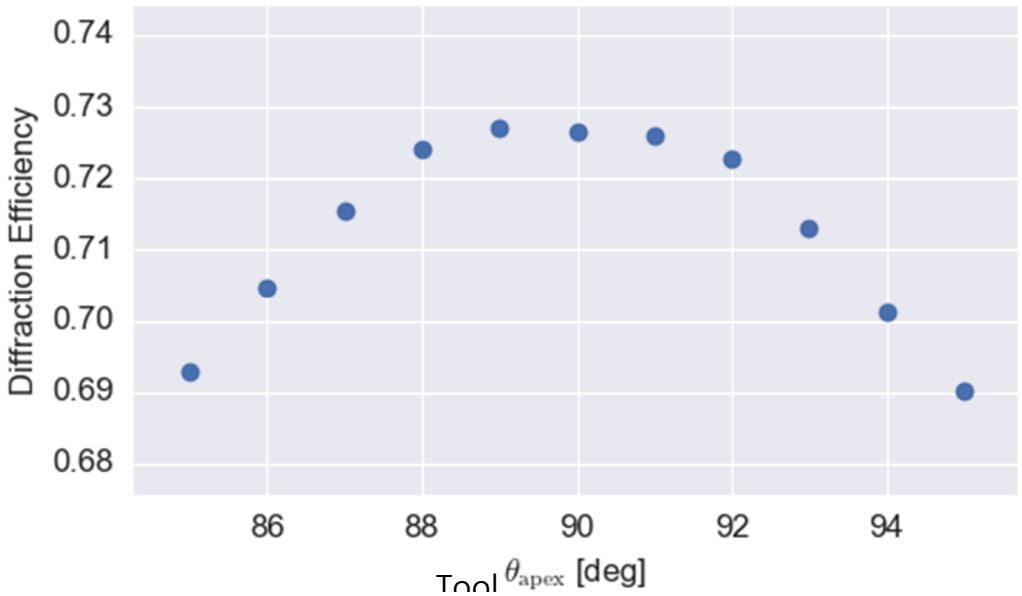

Figure 3. Rigorous Coupled Wave Analysis of the YJ grism is used to determine the optimal apex angle of the diamond tool. The calculation assumes uncoated ZnSe grooves, a perfect AR coating on the entrance face and TE polarization. A 90º angle is best.

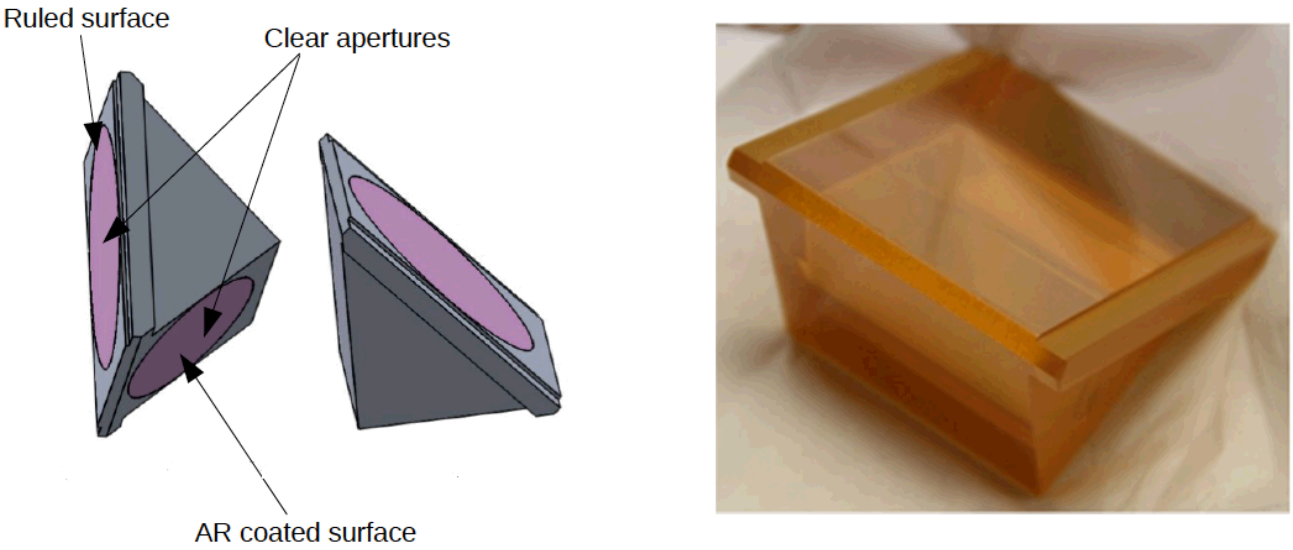

Figure 4. 3D drawings of the HK grism blanks are shown on the left and a photo of the actual ZnSe blank is on the right. The support rails can be clearly seen.

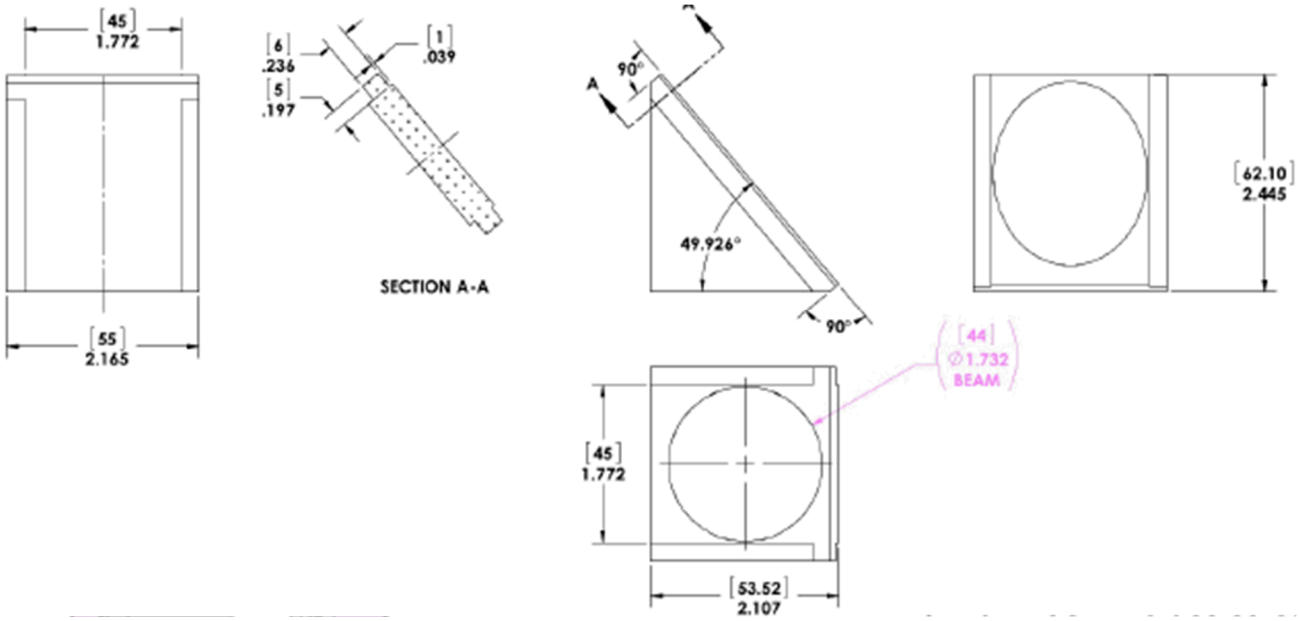

Figure 5. Mechanical details of the HK grism blanks are shown in the drawings above. The clear aperture is 44 mm diameter on the entrance face. The optical beam is 40 mm diameter or 90% of the clear aperture. The grating is ruled on the hypotenuse over a rectangular region, which just encompasses the elliptical clear aperture.

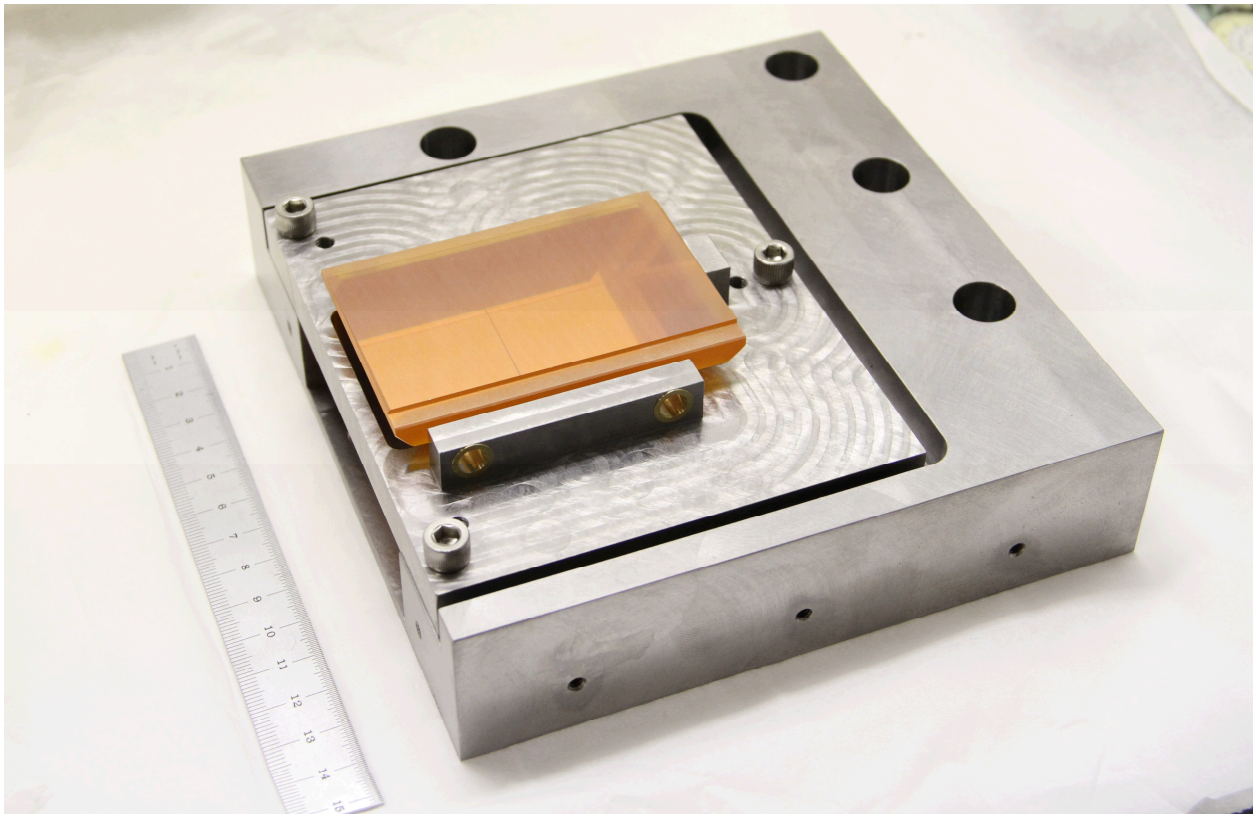

Figure 6. Photograph shows an HK grism blank installed in the low carbon steel machining fixture. A common base is used for both grisms. Only the support insert is changed.

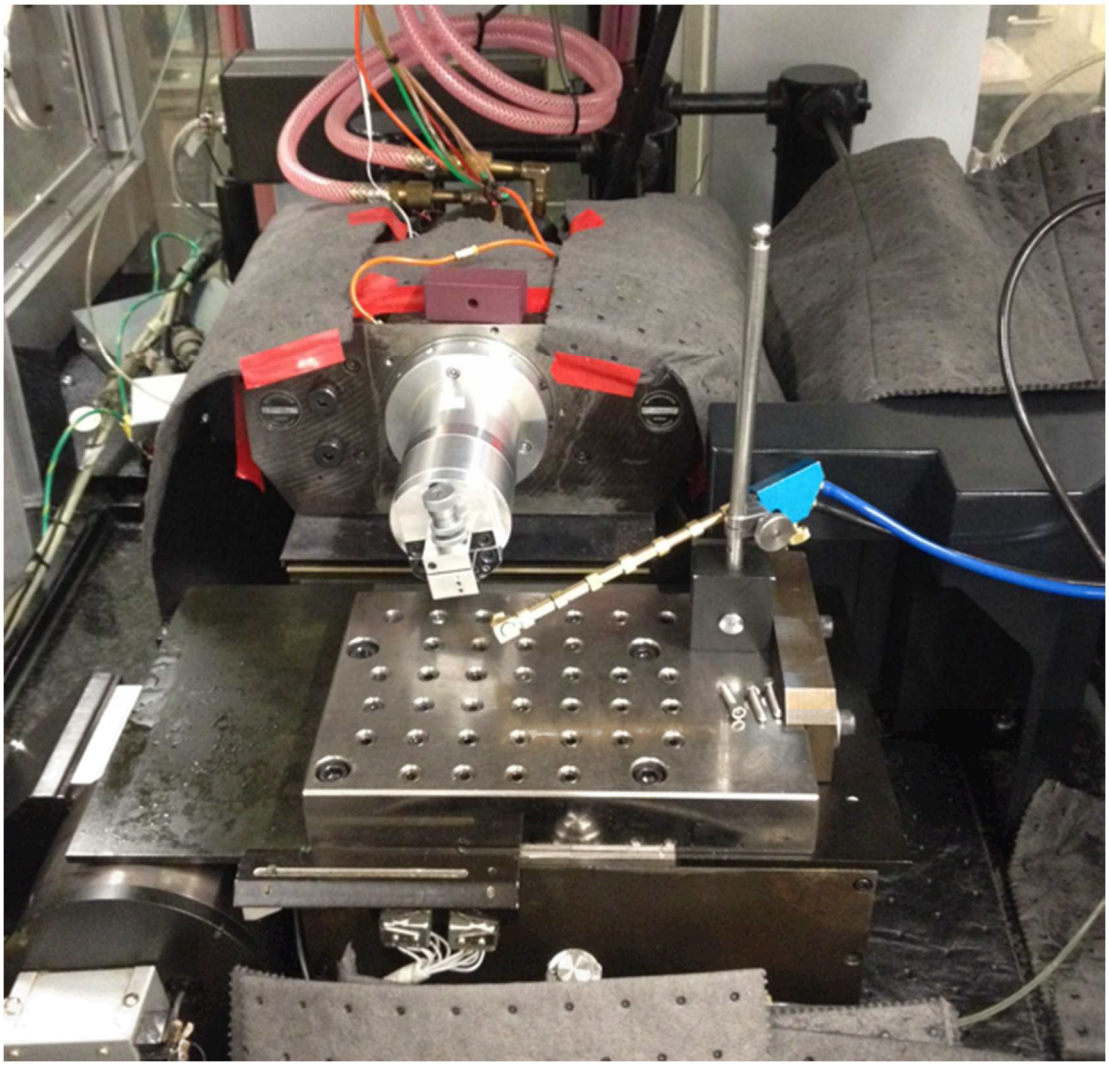

Figure 7. PERL II, LLNL's Precision Engineering Research Lathe

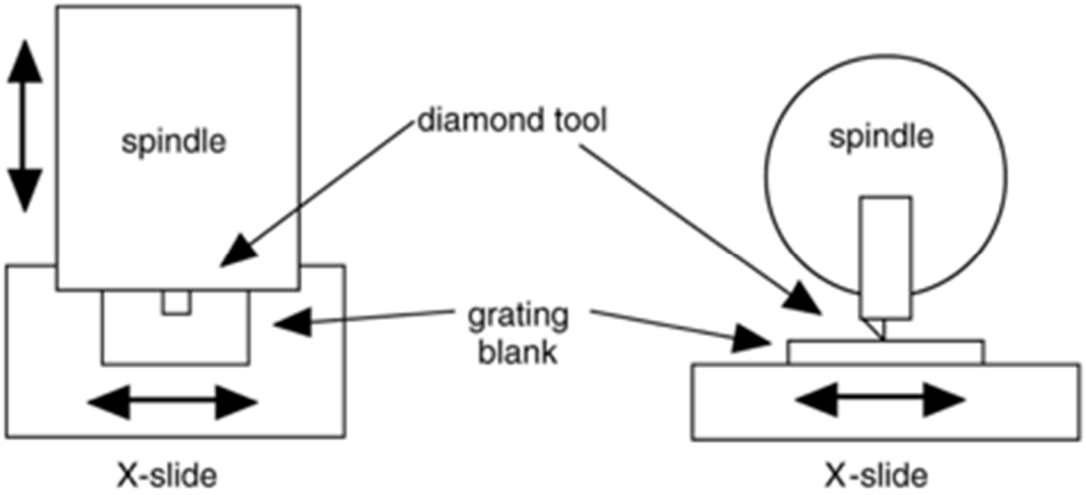

Figure 8. Cutting a grating with PERL II using flycutting. Z-axis is parallel to spindle motion; Y is in the vertical direction.

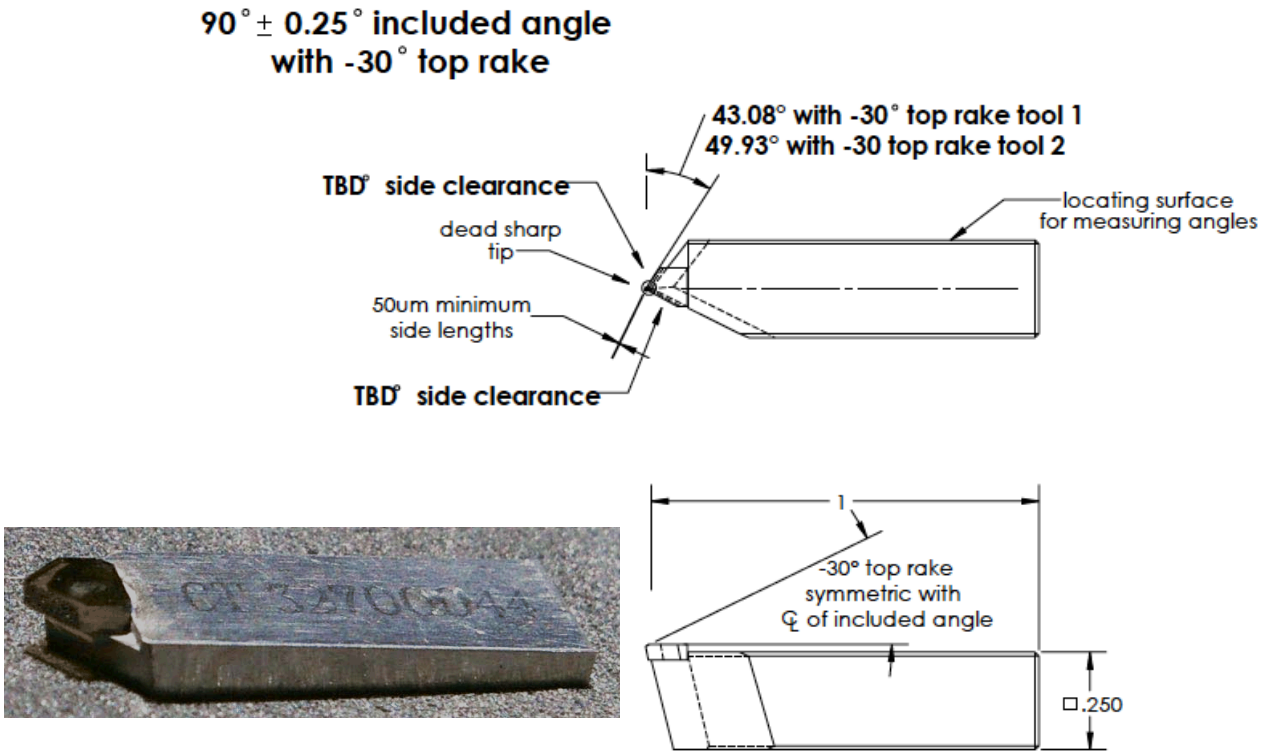

Figure 9. Detail of the diamond tools to be used to machine the grism

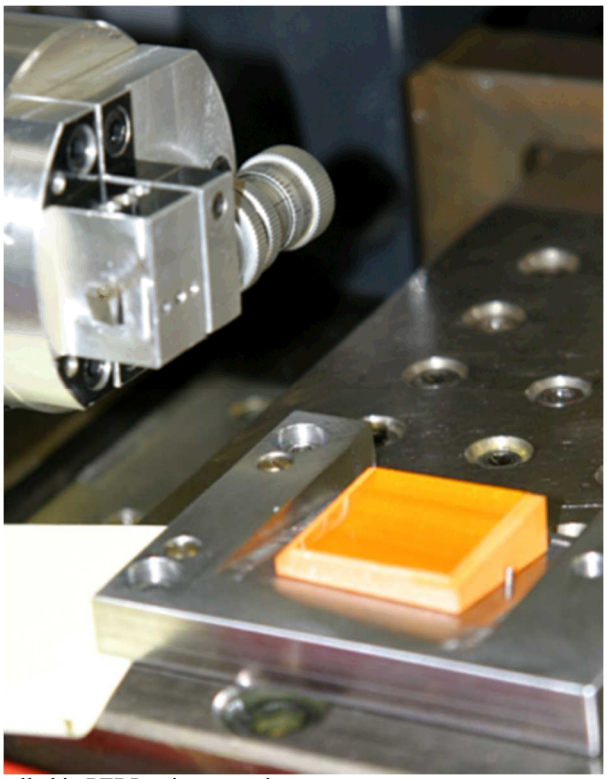

Figure 10. NIRISS grism blank installed in PERL prior to cutting